Correlating Structural Disorder, Paramagnetic Centers, and Dielectric Response in Cu^{2+}-Doped $BaO\text{-}In_2O_3\text{-}SiO_2$ Glasses

B. Ravi Kumar[1], L. Srinivasa Rao[2], A. Chitti Babu[3] and M. Srinivasa Reddy[1]*

[1] Department of Physics, Acharya Nagarjuna University , Nagarjua Nagar, A.P. -522510, India
[2] Department of Physics, Centre for Nanoscience and Technology, VNR Vignana Jyothi Institute of Engineering and Technology, Bachupalli, Hyderabad-5000090, Telangana, India
[3] Department of Physics, Sir. CR Reddy College of Engineering(A), Eluru-534007, A. P., India
***Corresponding Author, Mail: msreddy2004@gmail.com**

Abstract

Cu^{2+}-doped $40BaO\text{-}6In_2O_3\text{-}(54\text{-}y)SiO_2\text{-}yCuO$ glasses, where y ranges from 0.0 to 1.0 mol%, were prepared by the melt-quenching technique. The impact of Cu^{2+} doping in the presence of a TM on the structural, optical, paramagnetic, and dielectric properties of the glasses has been explored. The X-ray investigations confirmed the amorphous nature of the glasses doped with CuO, which reveals that CuO doping does not cause any crystallization in the glasses. Density and molar volume measurements confirmed that CuO doping causes compactness in the glasses. IR and Raman studies proved that the glasses doped with CuO have been depolymerized. The doped glasses showed d-d transitional bands in the visible and NIR regions due to Cu^{2+}. The optical bandgap and Urbach energy increased in the doped glasses. Electron spin resonance measurements confirmed the distorted octahedral environment for Cu^{2+} ions, with a monotonic increase in signal intensity with respect to CuO concentration. Dielectric studies indicated an enhancement in the dielectric constant and controlled dielectric loss behavior followed by space-charge and dipolar polarization mechanisms. The strong correlation of the ESR response with the dielectric properties underlines the important role of Cu^{2+}-induced defect states in tailoring the performance of multifunctional glasses.

Keywords: $BaO\text{-}In_2O_3\text{-}SiO_2$ glass, Cu^{2+} doping, Electron spin resonance, Optical bandgap,Dielectric properties, Structural disorder

1. Introduction

Oxide glasses are an important class of functional materials, and their technological relevance is extensive. This is due to their various possible applications in optoelectronic and photonic devices. Their ability to be structurally flexible, thermochemically stable, and possess the ability for various modifier and dopant ions to be integrated within the glass structure is what makes their technologically relevant properties visible. With this, they can be used for various applications, including optical fibers, lasers, and nonlinear optical devices [1,2]. Of different varieties of oxide glass, silicate glasses are found to be predominant owing to their superior chemical durability and high strength. Inclusion of alkaline earth oxides like BaO plays a significant role in influencing the physical and electrical properties of the glass [3, 4]. BaO acts basically as a network modifier: it breaks Si-O-Si linkages and provides non-bridging oxygens (NBOs), which have the potential to influence significantly such properties as density, optical absorption, dielectric polarization, and electrical conduction mechanisms. The $BaO\text{-}SiO_2$-based glass systems thus provide a convenient platform for the design of multi-functional glass materials with tunable structural and functional properties.Role of In_2O_3 in the Glass Network: Indium oxide is an amphoteric oxide that acts as a network former or modifier depending on the concentration and local coordination environment. In silicate glasses, In_2O_3 may substitute Si^{4+} sites and enter the network through In-O polyhedral units, while simultaneously modifying the local glass network structure. Such a balanced dual role enhances thermal stability and influences optical and dielectric behavior. In our previous study (Paper 1), systematic variation of the composition of the synthesized $BaO\text{-}In_2O_3\text{-}SiO_2$ glasses was

carried out with respect to the In_2O_3 composition over the entire range of the composition of the given glass system. It was demonstrated that the glass system with an In_2O_3 concentration of 6 mol% yields an optimal combination of structural stability, improved dielectric properties, and positive features of the optical response [11]. It was also noted that the glass system with an In_2O_3 content of 6 mol% possesses improved glass-forming ability and thermal stability, as well as a controlled degree of depolymerization under thermal treatment without crystallization. As such, the In_2O_3 content of the composition under the present consideration was fixed at a level of1.3 Transition Metal Ions in Glasses: The doping of oxide glasses with transition metal ions is a well-known technique for optimizing the optical, electrical, and sometimes magnetic properties of those materials. In the transition metal ions series, copper ions are very promising because they are highly active, have variable coordination geometry, and are paramagnetic too [13]. In general, characteristic d-d transitions of Cu^{2+} ions tend to appear in the visible and near infrared spectral region, making this ion of interest for investigations of ligand field and structural effects in glass matrices [14]. Moreover, the unpaired electron due to the Cu^{2+} ions makes them particularly useful for electron spin resonance spectroscopy. With the help of the ESR technique, various information related to the spectral properties of ions is obtained. More specifically, information related to the oxidation state and bonding environment of such ions is obtained. With the help of these properties, Cu^{2+} ions are considered particularly useful for establishing the correlation between glass structure changes and electronic structure.Although studies on copper-doped silicate glasses doped with Cu^{2+} ions have attracted considerable attention, very few studies have used optimized content of intermediate oxides and controlled doping with copper. In this study, the In_2O_3 content has been optimized at 6 mol%, which was determined from Paper 1. In addition, copper has been doped in the range from 0.0 to 1.0 mol%, where CuO is used as represented in reference [16]. The novelty of this present investigation resides in the comprehensive and correlated study of structural properties, optical properties, thermal properties, dielectric properties, and paramagnetic properties of Cu^{2+} doped $BaO\text{-}In_2O_3\text{-}SiO_2$ glasses system [17]. Among these properties and characteristics, particular emphasis has been given to ESR spectroscopic studies at correlated copper ions. XRD, FTIR, RAMAN, UV-Vis Spectroscopic studies, DSC studies, ESR spectroscopic studies, and dielectric measurements have provided comprehensive details regarding structural properties and their characteristics [18].Presently, the authors intend to prepare a series of Cu^{2+}-doped $40BaO\text{-}6In_2O_3\text{-}(54\text{-}y)SiO_2\text{-}yCuO$ glasses by the conventional melt-quenching technique and to perform systematic studies on the impact of Cu^{2+} incorporation on their structural, optical, thermal, and dielectric properties. Confirmation of the amorphous nature of the prepared glasses, along with an explanation of the changes in structure brought about by doping with Cu^{2+}, is done by analyzing density and molar volume and by performing vibrational spectroscopy. The main aim is centered on the optical behavior of the glasses by studying their absorption characteristics, optical bandgap, and Urbach energy as a function of CuO content. Moreover, electron spin resonance spectroscopy is carried out to understand the local electronic environment and the paramagnetic nature of Cu^{2+} ions. Finally, the effect of Cu^{2+} doping on dielectric constant and dielectric loss in a wide frequency range is evaluated to establish structure–property correlations and assess the potential of these glasses for optical and electronic applications.

2. Experimental Procedure

2.1 Glass Preparation: A series of Cu^{2+}-doped barium indium silicate glasses with the nominal composition $40BaO–6In_2O_3–(54–y)SiO_2–yCuO$ (y = 0.0–1.0 mol%) were prepared using the conventional melt-quenching technique. Analytical-grade $BaCO_3$, In_2O_3, SiO_2, and CuO (≥99.9% purity) were used as starting materials. Appropriate amounts of the raw materials were weighed according to the desired molar compositions and thoroughly mixed in an agate mortar to ensure homogeneity. The homogenized batches were transferred to high-purity alumina crucibles and melted in an electrically heated furnace at temperatures in the range of 1350-1450 °C for approximately 1 h, with intermittent stirring to achieve a uniform melt. The molten glass was then rapidly quenched by pouring onto a preheated stainless-steel plate and pressed with another plate to obtain bulk glass samples. To relieve internal stresses induced during quenching, the samples were immediately annealed at 400 °C for 3 h, followed by slow cooling to room temperature inside the furnace. The glasses obtained were transparent, homogeneous, and free from crystallization.

2.2 Characterizations:

2.2.1 X-ray Diffraction (XRD): The amorphous nature of the prepared glasses was confirmed by carrying out the X-ray diffraction analysis. For this analysis, patterns were created at room temperature using a PAN alytical X'Pert PRO. The device was supplied with Cu Kα radiation with a wavelength equal to 1.5406 Å. The scanning was carried out over a particular range of 2θ from 10 to 60 with a step size of 0.02. The absence of peaks would confirm the glassy nature [19].2.2.2 Density and Molar: The densities of the glass samples were determined using the Archimedes method by measuring the densities at room temperature, utilizing xylene as the immersion liquid. The densities were determined using relations, and the molar volume was then determined using the calculated densities and molecular weights of the glass samples. Data on densities and molar volume were used to verify the structural compactness and modification due to Cu^{2+} doping [20].
2.2.3 FTIR Spectroscopy: Fourier transform infrared spectra were acquired on a Bruker Tensor 27 FTIR spectrometer in the wavenumber range from 400 to 1600 cm^{-1} with a resolution of 4 cm^{-1}. Spectra were obtained using the KBr pellet technique. FTIR was performed for identifying some vibrational modes concerning Si-O-Si linkages, the non-bridging oxygen formation, and Cu–O related structural units in the glass network [21].2.2.4 Raman Spectroscopy: Raman spectra were recorded at ambient temperature with a Horiba Jobin Yvon LabRAM HR Evolution Raman spectrometer with a 532 nm diode-pumped solid-state laser as the excitation source. The recorded spectral range was between 200 and 1200 cm^{-1}. By Raman spectroscopy, information was obtained on the evolution of silicate structural units (Q^2, Q^3, and Q^4 species) and thus about network depolymerization effects caused by the incorporation of Cu^{2+} ions [22].2.2.5 Differential Scanning Calorimetry (DSC): Thermal properties of these glasses were investigated by using a thermal analyser 'NETZSCH DSC 404 F3 Pegasus'. Powdered glass samples were taken in 20 mg quantities and subjected to constant heating at a rate of 10 °C min^{-1} up to 900 °C from room temperature under a flowing nitrogen atmosphere. Glass transition temperature (Tg) and crystallization temperature (Tc) were revealed by scanning the DSC thermograms. The thermal stability parameter (ΔT = Tc - Tg) has been calculated for determining glass-forming ability [23].2.2.6 UV-**Vis Absorption Spectroscopy:** The optical absorption spectra were obtained with a Shimadzu UV-2600 spectrophotometer within a wavelength range of 200 to 1000 nm at room temperature. For obtaining the spectra, a glass sample was cut into a uniform thickness, then polished. The band gap energy values were obtained using Tauc's relation for indirect allowed transitions, while the Urbach energies were obtained to reveal information about structural disorder introduced by Cu^{2+} doping [24].2.2.7 Electron Spin Resonance: Electron Spin Resonance studies were carried out using a Bruker EMX-Plus X-band ESR spectrometer operating in the range of a 9.4 GHz frequency. The ESR spectra were taken at room temperature with a modulation frequency of 100 kHz. ESR studies were done to identify the oxidation state of the Cu^{2+} ions in the glass matrix [25].2.2.8 Dielectric measurements: The dielectric measurements were carried out using an Agilent 4294A Precision Impedance Analyzer with a frequency range from 10^2 to 10^6 Hz at room temperature. The electrodes were applied to both sides of the polished glasses using silver paste, and the dielectric constant (ε′) and dielectric loss (tan δ) were measured as a function of frequency to understand the polarization behavior of Cu^{2+} doped glasses [26].

3. Results and Discussion

3.1 X-ray Diffraction (XRD) Analysis: Figure 1 demonstrates the obtained X-ray diffraction patterns for $40BaO–6In_2O_3–(54–y)SiO_2–yCuO$ glasses with varying CuO content ranging from 0.0 to 1.0 mol% [27]. All glasses show a diffuse hump with a maxima located near 2θ = 28-32°, while none show any peaks indicative of crystalline order. The absence of crystalline peaks is a definitive characteristic for glass, which confirms the glass state for all the prepared glasses. It should be noted that no crystalline order is formed during glass preparation despite the incorporation of Cu^{2+} ions. The broad glass halo characteristics, which are typical in silicate-based glass systems, can be indexed to the short-range ordering of the Si-O-Si or In-O units. The absence of crystallization in the entire range of the Cu^{2+} doped glass system range suggests effective inclusion of the metal ions during the glass formation process. The characteristic feature of the broadened glass halo, observed in the entire range of the investigated glass system, suggests the modified role of the Cu^{2+} ions, as they act as an intermediate component in the system by retaining the disordered hexacoordination. Although it enters the glass network via the Cu-O bonds, the disordered hexacoordination of the Cu^{2+} is retained in the system.A close observation of the XRD patterns shows that there is a slight increase in the height of the amorphous peak as the CuO concentration is raised [27]. This may be ascribed to minor ordering effects in the glass structure, perhaps owing to the presence of non-bridging oxygens resulting from the incorporation of Cu^{2+} ions. Nevertheless, no alteration in the

position of the amorphous peak is observed; hence, it may be concluded that the average atomic distances in the glasses remain unaltered. More importantly, the absence of these crystalline structures at the highest concentration of CuO (1.0 mol%) is indicative of the good glass-forming ability of the $BaO\text{-}In_2O_3\text{-}SiO_2$ glassy system and its tolerance toward the doping of transition metals [28, 29]. Therefore, one can conclude the need for the stability of the structures for their application in optical and electronic devices, where the uniformity and amorphous nature of the structures play an important role in maintaining the functional properties of the materials. Overall, the XRD patterns ensure the amorphous nature of the Cu^{2+} ion-doped $40BaO\text{-}6In_2O_3\text{-}SiO_2$ materials.

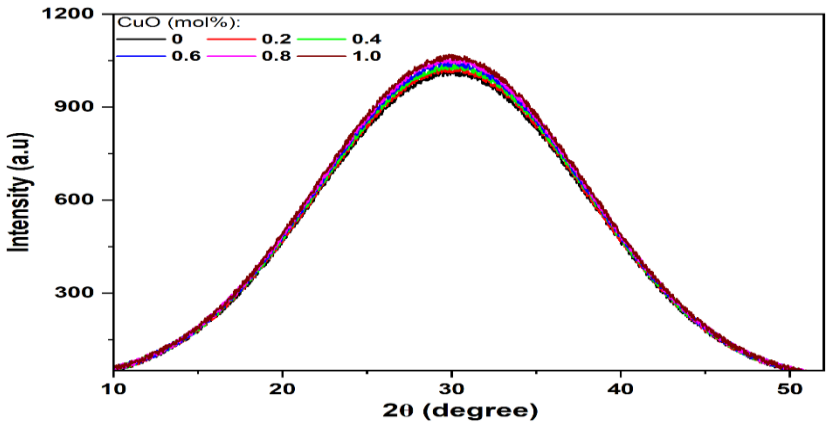

Figure 1. X-ray diffraction patterns of $40BaO–6In_2O_3–(54–y)SiO_2–yCuO$ glasses (y = 0.0–1.0 mol%), showing a broad amorphous halo and the absence of crystalline peaks, confirming the glassy nature of all compositions.3.2 Density and Molar Volume Analysis: Figure 2 presents variation of density and molar volume for the $40BaO–6In_2O_3–(54–y)SiO_2–yCuO$ glasses as a function of CuO content (y = 0.0-1.0 mol%) [30]. With the increase in the concentration of CuO, a systematic enhancement of density is obtained, whereas the molar volume exhibits a monotonic decrease correspondingly. The observed increase in density upon the addition of CuO can be understood to be primarily due to the replacement of lighter SiO_2 structural units by comparatively heavier CuO units within the glass network [31]. Copper ions, entering the glass matrix predominantly as Cu^{2+}, contribute higher molecular weight and enhanced mass packing in the structure. Besides this, Cu^{2+} ions prefer to occupy modifier or intermediate positions, leading to a more compact glass network. On the other hand, the observed reduction in molar volume suggests that progressive densification of the glass structure takes place [32]. This type of behavior indicates that the average interatomic spacing is reduced. This may be explained by the amount of additional non-bridging oxygens (NBOs), which are the result of the addition of CuO. The presence of the copper ion somehow alters the silicon-oxygen-silicon structure to include non-bridging oxygens, thus allowing the packing to be more optimal. The combined increase in density and decrease in molar volume further support the enhanced structural compactness as proposed by the amorphous nature of the XRD pattern (Figure 1) [30,31]. The results obtained from the density, molar volume, and XRD studies have further reinforced the efficacy of the role of CuO as a network modifier in the $BaO\text{-}In_2O_3\text{-}SiO_2$ glass system. The increased density of the system is likely to affect other physical properties, as discussed in the forthcoming sections [32].

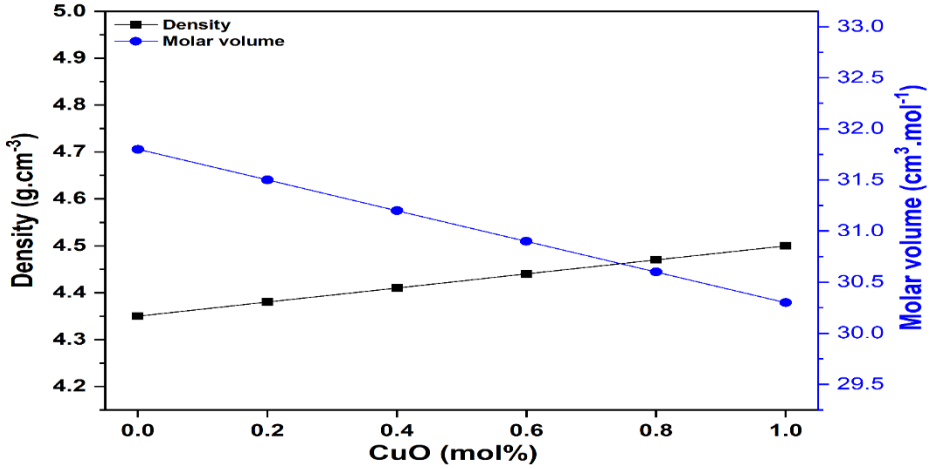

Figure 2. Variation of density and molar volume of $40BaO–6In_2O_3–(54–y)SiO_2–yCuO$ glasses as a function of CuO concentration (y = 0.0–1.0 mol%), showing an increase in density and a corresponding decrease in molar volume with increasing CuO content.3.3 FTIR Spectroscopy: Figure 3 displays the FTIR spectra of the $40BaO-6In_2O_3-(54-y)SiO_2-yCuO$ glasses scanned in the range of 400-1600 cm^{-1} [33]. All the glasses exhibit a wide absorption band with no sharp peaks, further confirming the amorphous nature of the glass matrix. This is consistent with the XRD findings [34]. The band centered at approximately 450-550 cm^{-1} is due to the bending modes of Si-O-Si groups along with the metal-oxygen bonds of Ba-O or In-O type [5]. On increasing the concentration of CuO, a slight increase in intensity along with broadening of the above-mentioned band is observed that might be due to the addition of Cu-O units. A distinct band at around ~750–850 cm^{-1} relates to the stretching vibrations of Si-O-Si bridges that relate more specifically to the characteristic Q^2 and Q^3 units of silicates [35]. The upward shift of the band with the addition of CuO points towards the progressive modification of the silicate network with the development of non-bridging oxygen. The wide band centered in the range of ~950-1100 cm^{-1} relates more specifically to the asymmetric stretching vibrations of $Si-O^-$ groups involving non-bridging oxygens. The increasing intensity of the band with an increased amount of CuO points towards the progressive development of non-bridging oxygen. This points towards the predominance of copper cations as modifiers of the silicate network, which break the Si-O-Si bridges and produce a depolymerized structure in the glass network. From the above discussion of the FTIR spectra of the examined glasses, it may be noted that the addition of CuO leads to considerable modifications in the structure of the explored $BaO-In_2O_3-SiO_2$ glass system due to an elevated level of network depolymerization characterized by the presence of non-bridging oxygen [33,34,35].

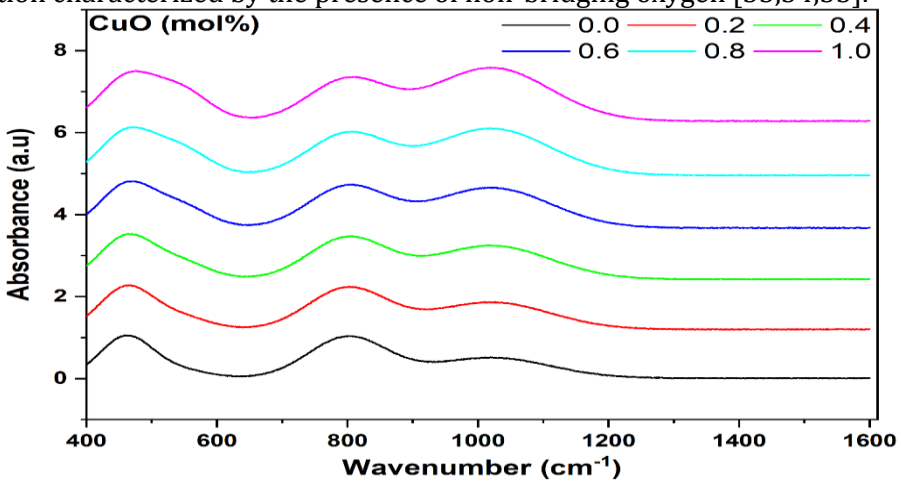

Figure 3. FTIR spectra of $40BaO–6In_2O_3–(54–y)SiO_2–yCuO$ glasses (y = 0.0–1.0 mol%) recorded in the range 400–1600 cm^{-1}, illustrating CuO-induced structural modifications and the formation of non-bridging oxygen sites within the glass network.

3.4. Raman Spectroscopic Analysis: Figure 4 presents the Raman spectra of $40BaO–6In_2O_3–(54–y)SiO_2–yCuO$ glasses with CuO concentrations ranging from 0.0 to 1.0 mol% [36]. All spectra exhibit broad and asymmetric Raman bands, which is a clear signature of the amorphous nature of the prepared glass samples, consistent with the XRD results discussed earlier [37]. The Raman spectra are dominated by two main broad bands centered approximately in the regions of 400-550 cm^{-1} and 850-1100 cm^{-1} [38]. The low-frequency band around 450 cm^{-1} is generally attributed to bending vibrations of Si-O-Si linkages and vibrations associated with modifier-related structural units, including contributions from Ba-O, In-O, and Cu-O polyhedra. The gradual rise of intensity together with the slight broadening of the bands with the rise of CuO concentration is indicative of the rise of structural disorder and the involvement of Cu^{2+} ions. The bands measured at 900-1100 cm^{-1} are characteristic of the Si-O stretching vibrations of various structural units of silicate glasses: Q^n species with n = 0-3. From the variation of the position of these bands with the rise of the CuO concentration, one can deduce that the glass network changes from the higher-connected units of type Q^3 to the lower-connected units of type Q^2 and Q^1, due to the rise of the NBOs as a result of the depolymerizing effect of the CuO modifier that cleaves the Si-O-Si bonds [37]. Furthermore, the increasing trend of Raman band intensification with increasing CuO content corroborates the pentavalent incorporation of Cu^{2+} ions as network modifiers as opposed to network formers [38]. The additional disorder from these Cu-O bonds, responsible for the localized vibrational modes, contributes to the significant alterations in bands observed. The Raman spectrum analysis agrees well with the FTIR analysis, confirming increasing network

depolymerization with the addition of CuO at the end of the spectrum. The Raman spectroscopy analysis manifestly proves the effect of Cu^{2+} ions on the short-range order of the $BaO–In_2O_3–SiO_2$ glass network by increasing the amount of NBOs and modifying the population of silicate Q species [36,37,38].

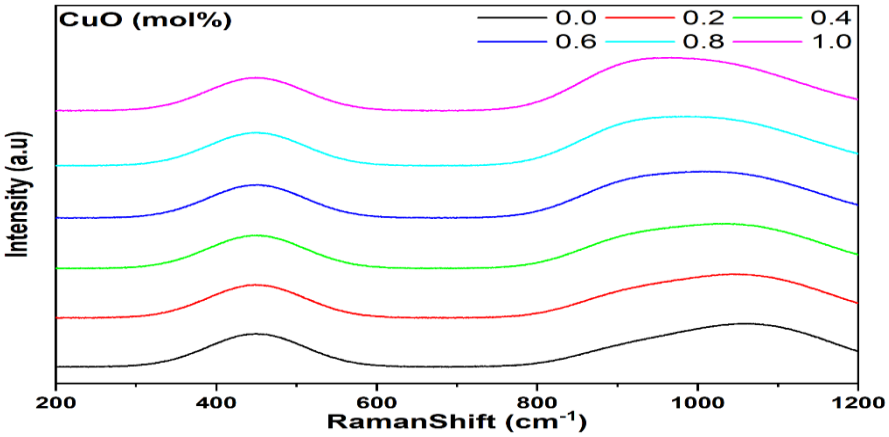

Figure 4: Raman spectra of $40BaO\text{-}6In_2O_3\text{-}(54\text{-}y)SiO_2\text{-}yCuO$ glasses with varying CuO content, ranging from y = 0.0 to 1.0 mol%, revealing the evolution of silicate Q species and network.

3.5 Differential Scanning Calorimetry (DSC) Studies: Differential Scanning Calorimetry was used to study the thermal properties of the engineered glass with the following composition: Cu^{2+}-doped $40BaO\text{-}6In_2O_3\text{-}(54–y)SiO_2\text{-}yCuO$. Their glass transition temperatures (Tg) and crystallization temperatures (Tc) are changing with each composition of CuO, and are displayed in Figure 5 [39]. Samples [40] exhibited the glassy character as well as the thermal stability as all composition showed an endothermic peak of glass transition, as well as an exothermic peak of crystallization. An observable trend is found with increasing CuO concentrations, as glass containing no CuO has Tg of approximately 535 °C, while glass containing 1.0 mol% CuO has Tg = 520 °C [3]. That Tg decrease of the glass is related to the Cu^{2+} ions acting as network modifiers to the silicate network. Silicate networks are formed with Si-O-Si structures, and the Cu^{2+} ions disrupt those structures, removing some oxygen thereby increasing the number of non-bridging oxygens. The glass network is less rigid overall with more non-bridging oxygens, due to an increase of non-bridging oxygens, less thermal energy is needed to relax the glass structure [39]. In a similar manner, the incorporation of CuO causes a decrease in the crystallization temperature (Tc). This means there is an increase in disorder and a decrease in the resistance to devitrification [40]. Cu^{2+} ions cause the localized disorder, which means more long range order fracturing can occur, leading to an enhancement in the ease of nucleation and growth of crystals at lower temperatures. Even though there is a decrease in both Tg and Tc, the separation of these temperatures ($\Delta T = Tc\text{-}Tg$) is still large enough in every case to demonstrate that there is still an adequate level of thermal stability to the glasses against crystallization [41]. The thermal trends show consistency with the structural changes deduced vis FTIR and Raman. more CuO content translates to more depolymerization of the glass network [39,40]. These findings show that with the ability to control Cu^{2+} doping, one can modify the thermal attributes of $BaO–In_2O_3–SiO_2$ glasses while retaining their glass-forming ability, vital for processing and device applications [39,41].

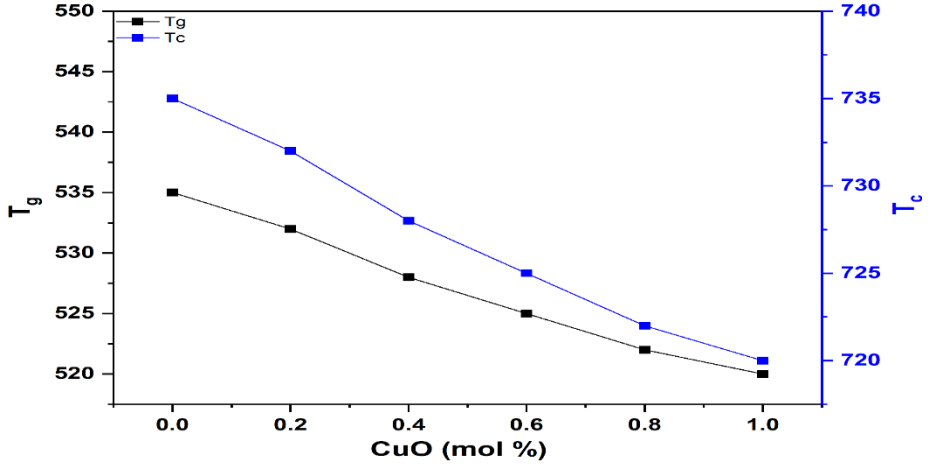

Figure 5. Variation of glass transition temperature (T_g) and crystallization temperature (T_c) as a function of CuO content for $40BaO–6In_2O_3–(54–y)SiO_2–yCuO$ glasses.

3.6 UV-Visible Optical Absorption Studies: Figure 6 presents the UV-visible absorption spectra of $40BaO–6In_2O_3–(54–y)SiO_2–yCuO$ glasses with CuO content varying from 0.0 to 1.0 mol% [42]. All samples exhibit a strong absorption band in the ultraviolet region below ~350 nm, which is attributed to charge transfer transitions from O^{2-} (2p) to metal cations present in the glass network [43]. The position of this absorption edge gradually shifts toward longer wavelengths with increasing CuO concentration, indicating a progressive narrowing of the optical bandgap. In addition to the UV absorption edge, a broad absorption band centered around ~750-850 nm is clearly observed in the visible–near infrared region for CuO-doped samples [44]. This band is absent in the undoped glass and becomes increasingly intense with increasing CuO content. The observed band is characteristic of Cu^{2+} ions in distorted octahedral or tetragonally elongated coordination environments and is assigned to the spin-allowed d-d transition $^2B_1g \rightarrow {}^2B_2g$ $/{}^2Eg/{}^2A_{1g}$. The monotonic increase in absorption intensity confirms the successful incorporation of Cu^{2+} ions into the glass matrix without phase separation or clustering.

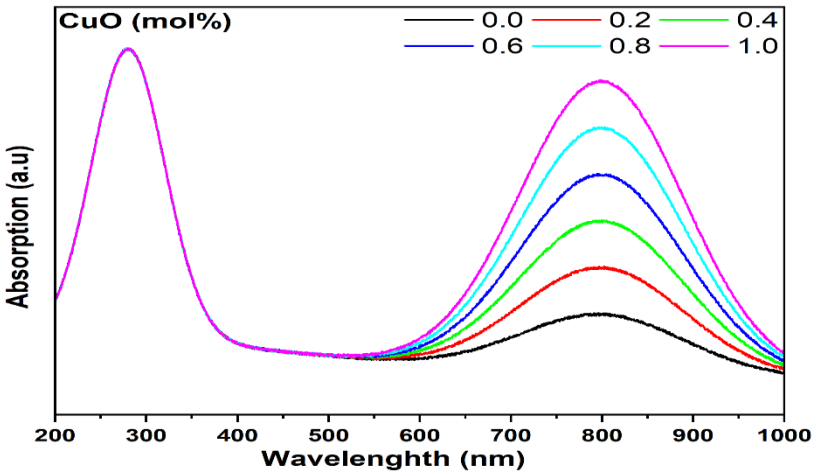

Figure 6. UV-visible absorption spectra of $40BaO–6In_2O_3–(54–y)SiO_2–yCuO$ glasses showing Cu^{2+}-related d-d transitions and absorption edge shift with increasing CuO content.Figure 6.1 illustrates the Tauc plots $(\alpha h\nu)^{1/2}$ as a function of photon energy ($h\nu$) for the investigated glasses, assuming indirect allowed electronic transitions, which is typical for amorphous oxide glasses [42]. The linear portions of the plots were extrapolated to intercept the energy axis to estimate the optical bandgap values [43]. The results reveal a systematic decrease in the optical bandgap from approximately 3.28 eV for the undoped glass to about 3.00 eV for the glass containing 1.0 mol% CuO [44]. This bandgap narrowing can be attributed to the introduction of localized Cu^{2+} 3d states within the forbidden gap and the formation of non-bridging oxygen (NBO) sites. The presence of these defect-related states enhances electronic polarizability and facilitates lower-energy electronic transitions, thereby reducing the bandgap. Figure 6.2 shows the compositional dependence of the optical bandgap (E_g) and Urbach energy (E_U) as a function of CuO concentration [42]. An apparent inverse correlation between Eg and E_U can be noted. With more CuO content, the optical bandgap continues to fall, and the Urbach energy rises from 0.20 eV → 0.30 eV. More Urbach energy indicates more structural disorder, as well as a greater number of localized states within the band-tail region [43]. This phenomenon is attributed to Cu^{2+}-induced distortion of the glass network, an increase of non-bridging oxygen (NBO) atoms, and disorder in the magnitudes of bond lengths and the angles between bonds. The significant drop in Eg, coupled with the rise in E_U, is an indication of CuO's strong network-modifying capability, adding defect states and thus changing the glass electronic structure [44]. The results from the UV-Vis spectra clearly indicate how the role of copper ion doping, denoted as Cu^{2+}, is vital in controlling the optical properties of the prepared $BaO/In_2O_3/SiO_2$ glasses system. The observation of unique d-d transitions, as well as bandgap and Urbach energy values, further indicate the incorporation of copper ions into the glass system. These findings are fully consistent with the FTIR and Raman analyses and provide a strong foundation for correlating optical behavior with ESR and dielectric responses in subsequent sections.

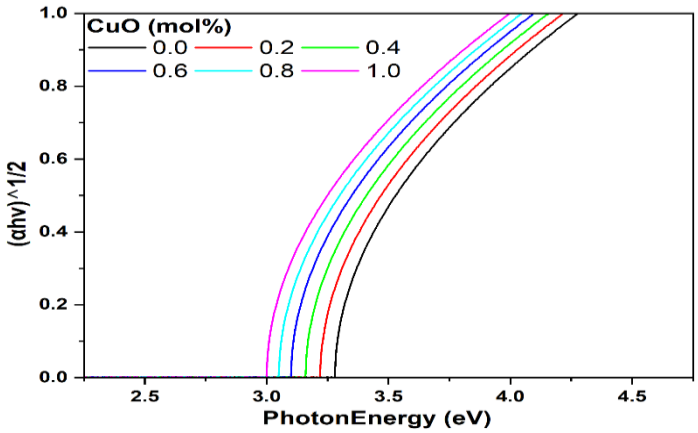

Figure 6.1. Tauc plots $(\alpha h\nu)^{1/2}$versus photon energy for CuO-doped glasses used to determine the optical bandgap.

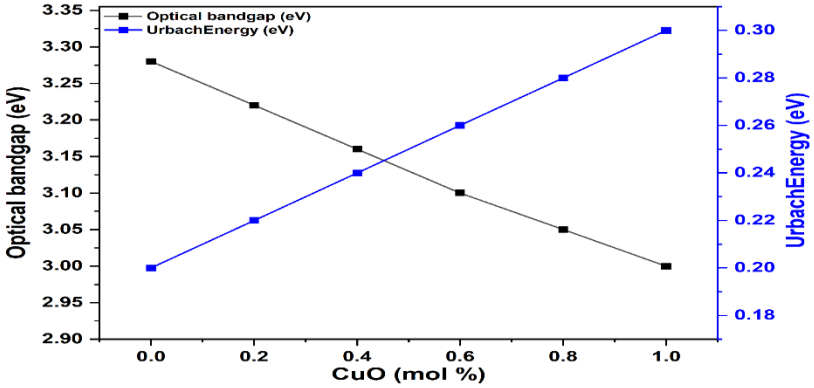

Figure 6.2. Variation of optical bandgap (E_g) and Urbach energy (E_U) as a function of CuO concentration in $BaO–In_2O_3–SiO_2$ glasses.3.7 Electron Spin Resonance (ESR) Analysis: Electron spin resonance spectroscopy was employed to investigate the local electronic environment and paramagnetic behavior of Cu^{2+} ions incorporated into the $BaO–In_2O_3–SiO_2$ glass network [45]. Figure 7 presents the first derivative ESR spectra recorded at room temperature for glasses containing different CuO concentrations (0.0-1.0 mol%) [46]. The undoped glass (0.0 mol% CuO) exhibits no distinct ESR signal, confirming the diamagnetic nature of the host glass matrix. Upon CuO incorporation, a well-defined resonance signal appears, whose intensity systematically increases with CuO content, clearly indicating the presence of paramagnetic Cu^{2+} ions ($3d^9$ configuration) [47]. The observed ESR spectra consist of a broad asymmetric signal centered around a magnetic field of ~3400 G, which is typical for Cu^{2+} ions in a distorted octahedral or tetragonally elongated coordination environment commonly encountered in oxide glasses.The absence of resolved hyperfine splitting indicates strong dipole–dipole interactions among the Cu^{2+} ions and structural disorder inherent in the amorphous glass network [45]. The gradual broadening and growth of the ESR signal with increasing concentration of CuO is due to the increased number of Cu^{2+} centers with enhanced spin–spin interactions. Moreover, the asymmetric line shape due to this reflects the coexistence of Cu^{2+} ions occupying slightly different local environments in the glass structure, influenced by varying degrees of network modification and non-bridging oxygen formation. In order to quantitatively investigate the paramagnetic behavior, the dependence of the ESR signal intensity on CuO content is presented in Figure 7.1 [46], in which the ESR signal intensity is collected from the peak-to-peak value of the derivative spectra. Generally, the ESR signal intensity shows almost linear behavior in its dependence on CuO content, indicating that the Cu^{2+} ions in the glasses have been doped without the phenomenon of clustering. Such results imply that the Cu^{2+} ions in the glasses have been doped homogeneously. The systematic enhancement of ESR signal intensity also favors the role of CuO as a network modifier, in which Cu^{2+} ions are mainly content with non-bridging oxygen sites resulting from the perturbation of Si-O-Si bonds [47]. The results are in good agreement with those of the FTIR and Raman spectra, which suggested an enhancement of network depolymerization with the addition of CuO. Overall, the ESR study presents strong indications of the successful doping of the $BaO–6In_2O_3–SiO_2$ glass system with Cu^{2+} ions, with ESR spectroscopy proving to be a powerful characterization tool for understanding the local environment of transition-metal ions in oxide glasses [45, 46, 47].

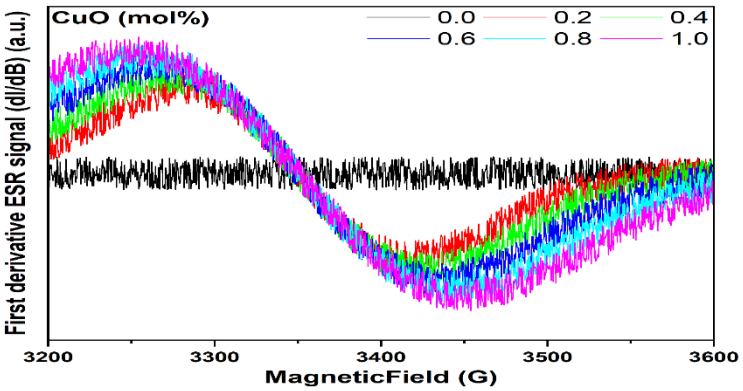

Figure 7. First Derivative ESR Spectra Recorded at Room Temperature for 40BaO-6In_2O_3-(54-y)SiO_2-yCuO Glasses as a Function of CuO Mol Percentage from 0.0 to 1.0 Mol Percent. Cu^{2+}

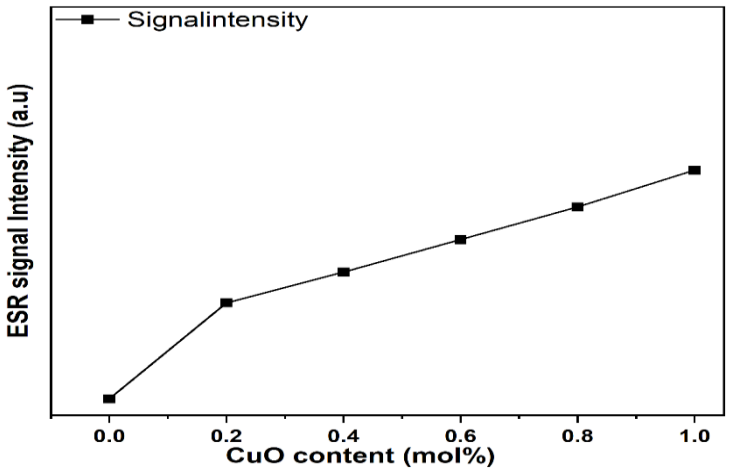

Figure 7.1. Variation of ESR signal intensity as a function of CuO content for 40BaO–6In_2O_3–(54–y)SiO_2–yCuO glasses, illustrating the systematic increase in paramagnetic Cu^{2+} centers with increasing CuO concentration.3.8 Dielectric Properties: The dielectric response of Cu^{2+}-doped 40BaO–6In_2O_3–(54–y)SiO_2–yCuO glasses was investigated as a function of frequency in the range of 10^2-10^6 Hz at room temperature [48]. The variation of dielectric constant (ε′) and dielectric loss (tan δ) with frequency for different CuO contents is presented in Figures 8 and 8.1, respectively [49].Dielectric constant (ε′): As shown in Figure 8, the dielectric constant exhibits a pronounced decrease with increasing frequency for all glass compositions [50]. At lower frequencies, ε′ attains relatively higher values, which can be attributed to the cumulative contribution of interfacial (Maxwell-Wagner), dipolar, ionic, and electronic polarizations. In this frequency regime, charge carriers like Cu^{2+} ions and non-bridging oxygen (NBO) sites can follow the applied alternating electric field. As the frequency increases continuously in a certain range, the dielectric constant reduces gradually and approaches a critical value that is nearly constant. This is due to the fact that the polarization response is slow compared to the oscillating electric field; interfacial and dipolar polarization mechanisms cannot usually respond to the electric field oscillations. These frequency changes in the dielectric constants are typical of disordered glassy systems [48]. In addition, for a given frequency, ε′ increases linearly with the increase of CuO content. This can be related to structural changes induced by the substitution of Cu^{2+} that enhances the formation of more non-bridging sites. The polarizability of Cu–O bonds and the mixed valence states Cu^{+}/Cu^{2+} facilitate localized charge displacement, hence enhancing dielectric activity. In good accordance, density and spectroscopic results have shown progressive depolymerization with CuO addition [50].

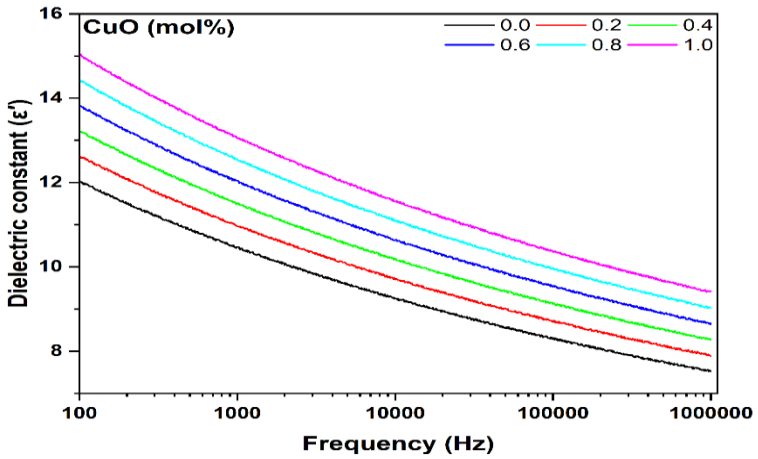

Figure 8. Frequency dependence of dielectric constant (ε′) for $40BaO–6In_2O_3–(54–y)SiO_2–yCuO$ glasses with Dielectric Loss (tan δ): Figure 8.1 shows the dielectric loss as a function of frequency [48]. In analogous ways to the behavior of the dielectric constant, the tan δ for all the composition decreases steeply with increased frequency. A greater value of dielectric loss at lower frequencies relates to energy losses due to space-charge polarization and hopping of charge carriers between localized states, especially between Cu^{2+} ions and defect centers [49]. As frequency is increased, dielectric loss is seen to decrease substantially. This decrease in dielectric loss proves that charge mobility is inhibited, resulting in the absence of relaxation loss. At higher frequency levels, the dielectric loss tangent assumes low values that are independent of frequency in the high-frequency region, indicating the presence of elastic polarization mechanisms with minimal losses over the broader frequency range [50]. Additionally, an enhancement in dielectric loss is seen as CuO concentration is increased, as demonstrated by the enhanced loss at increased frequencies. This can be ascribed to an improvement in charge carriers and structural defects due to a higher concentration of Cu^{2+} ions. However, due to the low value of dielectric loss at a higher frequency, it can be concluded that Cu^{2+} ions in the glass composition improve its insulating properties to a considerable extent, making them useful at increased frequencies for applications in dielectric and electronic properties [49, 50].

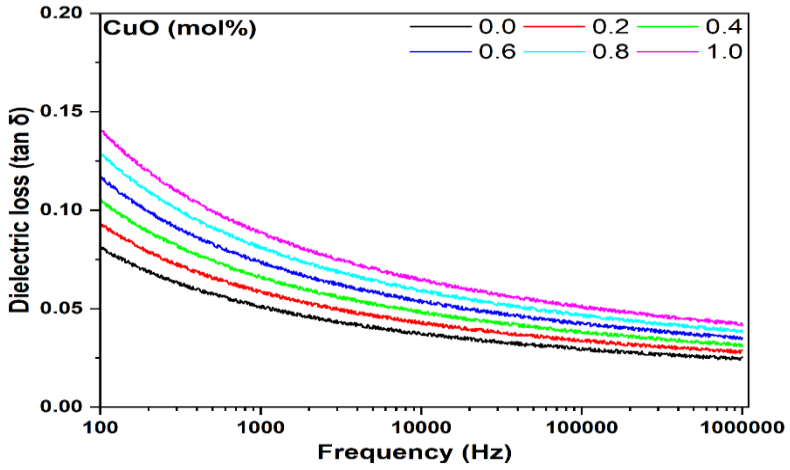

Figure 8.1: Frequency dependence of dielectric loss (tan δ) for glasses of the composition $40BaO–6In_2O_3–(54–y)SiO_2–yCuO$ However, by combining the results from XRD, ESR spectroscopy, and dielectric studies, an overall picture can be established regarding how Cu^{2+} ions influence the structural and electrical characteristics of $40BaO\text{-}6In_2O_3\text{-}(54\text{-}y)SiO_2\text{-}yCuO$ glass system. The combination of three techniques, when examined collectively and brings into focus how its structure-property relation is governed by Cu^{2+} ions in both modifier and electrical states. X-ray diffraction results verify the amorphous state of all compositions by the complete absence of sharp Bragg peaks and the presence of a broad diffuse feature at $2\theta \approx 28\text{-}32°$. The appearance of this feature in the diffractogram for all CuO concentrations is indicative of the fact that even Cu^{2+} incorporation of the order of 1.0 mol% does not produce crystallization. However, slight changes in the shape and height of the amorphous peak may be due to minor rearrangements within the glass

network structure. Such changes can be ascribed to continuous shifts from Si-O-Si structural units to Cu-O-Si and Cu-O linkages, which may result in increased network depolymerization.The impact of these structural changes is further highlighted in the ESR measurements, as it directly measures changes to the local electronic environment centered on Cu^{2+} ions. The first derivative signal, indicative of Cu^{2+}, is found to have a typical shape that corresponds to a disordered octahedral coordination environment, often tetragonally elongated. The increase in signal intensity with CuO concentration is a strong indicator that Cu^{2+} is incorporated into the glass lattice without any clustering or phase separation, as desired. The broadening of the signal is indicative of a distribution in the local environment, consistent with the disordered arrangement of glass networks identified through XRD. Significantly, the progressive increase in ESR signal intensity with CuO concentration points to an increased population of paramagnetic Cu^{2+} species. The species are likewise responsible for defect generation through non-bridging oxygen generated during network depolymerization. The non-bridging oxygen acts as charge carriers, enabling hopping conduction due to an externally applied field. Therefore, it can be concluded that ESR data point to a direct microscopical link between coordination chemistry and electrical properties.Such structural and electronic changes observed undergo a great correlation with the changes observed with the glass materials presented in terms of their dielectric properties. An increase in dielectric constants is observed with an increase in the concentration of CuO due to a corresponding increase in the percentage of non-bridging oxygen. Also, space charge and dipole polarization occur predominantly only at low frequency values because of the presence of Cu^{2+} ions as impurities. As a result, the dielectric constants are observed to be high. Once the value of frequency increases, there is an observation of dielectric dispersion. Similarly, the increase in dielectric loss value with CuO content can be explained by the improved dissipation of energy due to charge carrier hopping among localized Cu^{2+} states. Similarly, the reducing trend in dielectric loss values with increasing frequency confirms the dominant role of low-frequency polarization in relaxation losses. Despite the improvement in dielectric loss values with CuO content, low values of tan δ in the high-frequency region show good dielectric stability. Overall, the strong correlations among the XRD, ESR, and dielectric results demonstrate the effectiveness of Cu^{2+} doping in creating control over structural disorder without sacrificing the amorphicity of the system, all the while increasing the amount of electrical polarization by utilizing defect-based phenomenon. The Cu^{2+} ions have been extremely effective as probes of the material and as active players in the dielectric properties. The $BaO\text{-}In_2O_3\text{-}SiO_2$ glasses have the potential to be used in technology because of the synergistic effects that the structural flexibility, the paramagnetic functionality, and the dielectric properties offer.

4.0 Discussion:

The results of the studies carried out using XRD, ESR spectroscopy, and dielectric techniques give an insight into the understanding of how copper ions influence the corresponding $40BaO–6In_2O_3–(54–y)SiO_2–yCuO$ glasses. A study of these techniques, as already indicated, suggests a structure–property relationship in which copper ions act as a network modifier as well as an electrically active species. X-ray diffraction studies verify the amorphous nature of all the compositions by the absence of sharp Bragg peaks and the appearance of a broad diffuse band around 2θ, which is typically around 28-32°. The presence of this band in all the compositions indicates that adding CuO in various concentrations does not cause the material to crystallize. The small changes in the height and width of the band may be due to changes in the glass network following the introduction of Cu^{2+} ions. The changes may have been caused by the progressive replacement of Si-O-Si by Cu-O-Si linkages. This results in network depolymerization and increased disorder.These structural changes are even more apparent in ESR results, which probe the local electronic environment of the Cu^{2+} ions. The ESR spectra present a characteristic first-derivative signal, typical of Cu^{2+} ions in

distorted octahedral or tetragonally elongated coordination. The systematic increase in ESR signal intensity with the addition of CuO confirms that Cu^{2+} ions have been successfully incorporated into the glass matrix without clustering or phase separation. Broad linewidths together with an asymmetric shape of the signal point out the distribution of Cu^{2+} sites, which is in accordance with a disordered nature of the glass network evidenced from XRD. Importantly, the gradual enhancement of ESR intensity with the CuO concentration reflects the increase in the population of the paramagnetic Cu^{2+} centers and the defect-related states. These centers are closely associated with non-bridging oxygen atoms created during network depolymerization. Such defects act as localized charge carriers, facilitating hopping conduction under an applied electric field. Thus, the results from ESR establish a direct microscopic link between Cu^{2+} coordination, defect generation, and electrical activity of this glass system.This evolution in structure and electronic properties is

reflected very prominently in the dielectric properties of the glasses. The observed variation in dielectric constant with increasing concentration of CuO may be directly related to an increase in non-bridging oxygen and polarizability of the Cu–O bonds. Space charge and dipolar polarizations would be prominent at low frequencies due to the presence of Cu^{2+}, and hence, the dielectric constant is high. With increasing frequencies, the inability of the polarizations to respond to the alternating field would lead to dielectric dispersion. Also, the increase of dielectric loss with the concentration of CuO is due to greater energy loss due to hopping of charge carriers between localized Cu^{2+} ions. The reduction of dielectric loss with frequency is due to the lower charge carriers at higher frequencies. The results indicate that the relaxation loss is mainly due to low-frequency polarization. Even though the dielectric loss increases with the concentration of CuO, low values of tan δ at higher frequencies are responsible for the dielectric stability of the glasses. Overall, the evidence for strong correlation between the results from the XRD, ESR, and dielectric studies confirms that the structural disorder induced by Cu^{2+} doping is clearly controlled without being detrimental to amorphicity, and that the respective electrical polarization is augmented. The ions are seen to function both as effective probes for structural ordering and as active players in electrical polarization, which confirms the high potential for tuning the $BaO–In_2O_3–SiO_2$ glass system for various technological applications.

5. Conclusion

Systematic studies on Cu^{2+} ions doped into $40BaO–6In_2O_3–(54–y)SiO_2–yCuO$ glasses to explore the effects of transition metal ions on the optical properties of glasses has been done. X-ray diffraction confirmed the glasses retained their amorphous structure over the entire range. This shows that the addition of CuO into the glasses does not contribute to their crystallization, but it induces order within the disordered network. Analysis of density measurements and molar volume indicates the gradual compaction of the glass matrix as a result of increasing content of CuO, owing to the presence of Cu–O bonds and the generation of non-bridging oxygen species. In this regard, the results based on the FTIR and Raman spectroscopic studies confirm the structural changes associated with the depolymerization of the silicate matrix together with the evolution of Q species with reduced connectivity. These results establish the effectiveness of Cu^{2+} ions as modifiers in the optimized In_2O_3-containing glass matrix. Moreover, the optical absorption studies have demonstrated characteristic bands of d-d transitions of Cu^{2+} ions in the visible region, and optical bandgap has decreased, whereas Urbach energy increased systematically upon increasing the concentration of CuO. These studies confirm enhanced structural disorder and localized electronic states in the bands. ESR spectra directly confirmed the presence of Cu^{2+} ions in structurally disturbed coordinations, which were either distorted octahedral or tetragonally elongated, and intensity also increased systematically with an increase in the concentration of CuO.The dielectric measurements indicated that the doping of Cu^{2+} highly enhanced the dielectric constant with relatively low dielectric loss at higher frequencies. The relaxation behavior of such a dielectric dispersion was determined by the space-charge and dipolar polarization mechanisms related to Cu^{2+} ions and non-bridging oxygen defects. The strong correlation between the ESR signal intensity and the dielectric response underlines the decisive role of defect states related to Cu^{2+} ions in the process of electrical polarization and energy dissipation. In general, this work has proved that the optimum fixation of In_2O_3 and controlled Cu^{2+} doping is an effective approach for tuning the structure-function properties of $BaO–SiO_2$ glass. Overall, improved optical activity, paramagnetic

response, and enhanced dielectric performance make these glasses suitable for advanced dielectric components, optoelectronic devices, and a plethora of glass-based applications.

References:

1. *Shelby, J.E., 2020. Introduction to glass science and technology. Royal society of chemistry.*
2. *Varshneya, A.K., 2013. Fundamentals of inorganic glasses. Elsevier.*
3. *Doremus, R.H., 2001. Diffusion of reactive molecules in solids and melts. John Wiley & Sons.*
4. *Lines, M.E. and Glass, A.M., 2001. Principles and applications of ferroelectrics and related materials. Oxford university press.*
5. *Griscom, D.L., 1980. Electron spin resonance in glasses. Journal of Non-Crystalline Solids, 40(1-3), pp.211-272.*

6. McMillan, P., 1984. Structural studies of silicate glasses and melts—applications and limitations of Raman spectroscopy. American Mineralogist, 69(7-8), pp.622-644.
7. Moustafa, Y.M. and El-Egili, K., 1998. Infrared spectra of sodium phosphate glasses. Journal of non-crystalline solids, 240(1-3), pp.144-153.
8. Karabulut, M., Melnik, E., Stefan, R., Marasinghe, G.K., Ray, C.S., Kurkjian, C.R. and Day, D.E., 2001. Mechanical and structural properties of phosphate glasses. Journal of Non-Crystalline Solids, 288(1-3), pp.8-17.
9. Safieddine, F., Hassan, F.E.H. and Kazan, M., 2024. Thermal properties of In2O3 and α-Ga2S3 compounds. Solid State Communications, 391, p.115629.
10. Karazhanov, S.Z., Ravindran, P., Vajeeston, P., Ulyashin, A., Finstad, T.G. and Fjellvåg, H., 2007. Phase stability, electronic structure, and optical properties of indium oxide polytypes. Physical Review B—Condensed Matter and Materials Physics, 76(7), p.075129.
11. Ibrahim, S., Khattari, Z.Y. and Mahdy, E.A., 2025. Impact of In2O3 content on the structural, thermal, and mechanical hallmarks of Na_2O-BaO-ZnO-Fe_2O_3-P_2O_5 glass systems. Journal of Materials Science: Materials in Electronics, 36(10), p.601.
12. Rao, K.J., 2002. Structural chemistry of glasses. Elsevier.
13. Bishay, A., 1970. Radiation induced color centers in multicomponent glasses. Journal of Non-Crystalline Solids, 3(1), pp.54-114.
14. Donald, I.W., 2010. Waste immobilization in glass and ceramic based hosts: radioactive, toxic and hazardous wastes. John Wiley & Sons.
15. Fox, K.E., Furukawa, T. and White, W.B., 1982. Transition metal ions in silicate melts. Part 2. Iron in sodium silicate glasses. Phys. Chem. Glasses;(United Kingdom), 23(5).
16. Elliott, S.R., 1990. Physics of amorphous materials. (No Title).
17. Bergo, P., Pontuschka, W.M., Prison, J.M., Motta, C.C. and Martinelli, J.R., 2004. Dielectric properties of barium phosphate glasses doped with transition metal oxides. Journal of non-crystalline solids, 348, pp.84-89.
18. Lin, B.N. and Shih, Y.T., 2024. Temperature and frequency-dependent dielectric properties prediction of oxide glasses by machine learning. Ceramics International.
19. Cullity, B.D. and Smoluchowski, R.J.P.T., 1957. Elements of X-ray Diffraction. Physics Today, 10(3), pp.50-50.
20. Rüssel, C., 1999. Introduction to glass science and technology. Zeitschrift für Physikalische Chemie, 208(1-2), pp.292-293.
21. Moustafa, Y.M. and El-Egili, K., 1998. Infrared spectra of sodium phosphate glasses. Journal of non-crystalline solids, 240(1-3), pp.144-153.
22. Sitarz, M., 2011. The structure of simple silicate glasses in the light of Middle Infrared spectroscopy studies. Journal of non-crystalline solids, 357(6), pp.1603-1608.
23. Höland, W. and Beall, G.H., 2012. Glass-ceramic technology (Vol. 346). Hoboken, NJ: Wiley.
24. Tauc, J. ed., 2012. Amorphous and liquid semiconductors. Springer Science & Business Media.
25. Takada, A., Conradt, R. and Richet, P., 2013. Residual entropy and structural disorder in glass: A two-level model and a review of spatial and ensemble vs. temporal sampling. Journal of non-crystalline solids, 360, pp.13-20.
26. Beeby, J.L., 1985. Physics of Amorphous Materials.
27. Zarzycki, J., 1991. Glasses and the vitreous state (No. 9). Cambridge university press.
28. Zachariasen, W.H., 1932. The atomic arrangement in glass. Journal of the American Chemical Society, 54(10), pp.3841-3851.
29. Greaves, G.N. and Sen, S., 2007. Inorganic glasses, glass-forming liquids and amorphizing solids. Advances in physics, 56(1), pp.1-166.
30. Wong, J. and Angell, C.A., 1976. Glass: structure by spectroscopy. (No Title).
31. Henderson, G.S., 2005. The structure of silicate melts: a glass perspective. The Canadian Mineralogist, 43(6), pp.1921-1958.
32. Bray, P.J., Geissberger, A.E., Bucholtz, F. and Harris, I.A., 1982. Glass structure. Journal of Non-Crystalline Solids, 52(1-3), pp.45-66.
33. Mysen, B.O., 1990. The role of aluminum in depolymerized, peralkaline aluminosilicate melts in the systems Li_2O–Al_2O_3–SiO_2, Na_2O–Al_2O_3–SiO_2 and K_2O–Al_2O_3–SiO_2. Am. Mineral, 75, pp.120-134.
34. Neuville, D.R., Cicconi, M.R., Blanc, W. and Lancry, M., 2021. Applications of Raman spectroscopy, a tool to investigate glass structure and glass fiber. Fiberglass Science and Technology: Chemistry, Characterizations, Processes, Modeling, Applications, and Sustainability.

35. Henderson, G.S., 2005. The structure of silicate melts: a glass perspective. The Canadian Mineralogist, 43(6), pp.1921-1958.
36. Hrubý, A., 1972. Evaluation of glass-forming tendency by means of DTA. Czechoslovak Journal of Physics B, 22(11), pp.1187-1193.
37. Ray, C.S., Yang, Q., Huang, W.H. and Day, D.E., 1996. Surface and internal crystallization in glasses as determined by differential thermal analysis. Journal of the American Ceramic Society, 79(12), pp.3155-3160.
38. Hägg, G., 1935. The vitreous state. The Journal of Chemical Physics, 3(1), pp.42-49.
39. Clark, A.H., 1967. Electrical and optical properties of amorphous germanium. Physical Review, 154(3), p.750.
40. Dimitrov, V. and Sakka, S., 1996. Electronic oxide polarizability and optical basicity of simple oxides. I. Journal of Applied Physics, 79(3), pp.1736-1740.
41. Zamyatin, O.A., Plotnichenko, V.G., Churbanov, M.F., Zamyatina, E.V. and Karzanov, V.V., 2018. Optical properties of zinc tellurite glasses doped with Cu2+ ions. Journal of Non-Crystalline Solids, 480, pp.81-89.
42. Hansen, S. and Müller-Warmuth, W., 1991. JR Pilbrow: Transition Ion Electron Paramagnetic Resonance, Clarendon Press, Oxford 1990. ISBN 0-19-855214-9. 717 Seiten, Preis:£ 85.–.
43. Abragam, A. and Bleaney, B., 2012. Electron paramagnetic resonance of transition ions. OUP oxford.
44. Suresh, S., Babu, J.C. and Chandramouli, V., 2005. ESR, infrared and optical absorption studies of Cu^{2+} ion doped in xB_2O_3−(100− x) TeO_2 glass system. Physics and chemistry of glasses, 46(1), pp.27-30.
45. Jonscher, A.K., 1999. Dielectric relaxation in solids. Journal of Physics D: Applied Physics, 32(14), p.R57.
46. Mott, N.F. and Davis, E.A., 2012. Electronic processes in non-crystalline materials. OUP Oxford.
47. Sidebottom, D.L., 1999. Universal approach for scaling the ac conductivity in ionic glasses. Physical review letters, 82(18), p.3653.
48. Vaish, R. and Varma, K.B.R., 2011. Electrical relaxation and transport in 0.5 Cs_2O-0.5 Li_2O-$3B_2O_3$ glasses. IEEE Transactions on Dielectrics and Electrical Insulation, 18(1), pp.155-161.
49. Sidebottom, D.L., 1999. Universal approach for scaling the ac conductivity in ionic glasses. Physical review letters, 82(18), p.3653.
50. Salman, F., 2013. Dielectric characteristics of CuO-Na_2O-SiO_2 glasses with cole-cole plots technique and ac conductivity study. Glass Physics and Chemistry, 39(2), pp.150-154.